Simulation Inquisition of Noise Dissolving Algorithm Hinge on Triple Threshold Statistical Detection Filter for Random Intensity Impulse Noise Situation

Vorapoj Patanavijit[1] and Kornkamol Thakulsukanant[2]

ABSTRACT: This primary aim of this theoretical paper is to investigate the efficacy of a noise dissolving algorithm hinging on a TTSD (Triple Threshold Statistical Detection) filter originated in 2018 for applying to fixed intensity impulsive noise at high density (75%-95%). It has the highest efficacy for dissolving impulse noise exclusively on dense distributions. As a result, there are three essential contributions: 1). the exhaustive explanation of the TTSD filter algorithm, 2). the computation examples, 3). the calculation simulation of noise apprehension correctness and overall comparative simulation of noise dissolving effectiveness for RIIN at all densities (5%-90%). For TTSD filter, three malleable offsets that are the complementary requirement are employed in the TTSD filter that can adequately resolve the limitation of the antecedent noise dissolving algorithms. The first malleable offset is calculated for determining the noise characteristic of all elements using mathematical verification. Next, the second malleable offset is calculated for determining another noise characteristic by using normal distribution mathematical verification (the average value and standard deviation value). Later, the third malleable offset is calculated for determining another noise characteristic by using the quartile mathematical verification (median value). In the simulation inquisition, the bountiful standard portraits that are desecrated by RIIN (Random Intensity Impulse Noise) with many dense distributions are initially investigated from a noise apprehension correctness performance point of view. Later, these portraits are denoised by a noise dissolving algorithm hinging on TTSD, which is compared with numerous state-of-art noise dissolving algorithms such as Median filter (SMF), Mean/Gaussian filter, the adaptive median filter (AMF) technique, and Bilateral filter (BF), in both quantitative and quality indexes.

Keywords: TTSD (Triple Threshold Statistical Detection) Filter, Mean Filter, Median Filter, Adaptive Median Filter (AMF), Bilateral Filter (BF)

DOI: 10.37936/ecti-cit.2021153.240960

Article history: received October 5, 2020; revised January 23, 2021; accepted August 8, 2021; available online October 21, 2021

1. THE INTRODUCTION OF NOISE DESSOLVING ALGORITHMS FOR IMPULSIVVE NOISE

In the last three decades, many algorithms [1-20] that hinge on distinctive techniques have been investigated and evolved for noise apprehension and noise dissolving [10-20] in order to restore profaned portraits because there are great requirements for high quality portraits, which have been used in modern complex applications [1-4] such as medical imaging [7-9], remote sensing [6], super resolution (SR) [5], facial expression identification, smart CCTV system, etc. Initially, the MF (median filter) technique [21] was investigated and it has evolved since 1975 for FIIN (Fix-Intensity Impulse Noise). However, this MF technique dissolves every portrait dot (in both noise-free dots and noisy dots) so many fine details of dissolved portraits are lost. Later, the AMF (adaptive median filter) technique [22] which evolved from the MF technique with adaptive window size was in-

[1,2]The authors are with Assumption University of Thailand, Bangkok, Thailand., E-mail: Patanavijit@yahoo.com and kthakulsukanant@yahoo.com

vestigated since 1994. AMF has better effectiveness for FIIN. As a result, there are many contemporary noise dissolving algorithms [23-31] which can usually be separated into two essential processes: noise apprehension and noise dissolving. They have been investigated and evolved during this period of time. As a result, the TTSD filter technique [31] has been investigated and evolved for applying on fixed intensity impulsive noise at high density (75%-95%). It has a high dissolving effectiveness because the TTSD filter can adequately resolve the limitation of the antecedent noise dissolving algorithms. No research paper investigates the performance of TTSD when the TTSD filter is applied on RIIN at other noise densities. The TTSD filter has three malleable offsets that are the complementary requirement. The first malleable offset is calculated for determining the noise characteristic of all elements using mathematical verification. Next, the second malleable offset is calculated for determining another noise characteristic using the normal distribution mathematical verification (the average value and standard deviation value). Later, the third malleable offset is calculated for determining the another noise characteristic using the quartile mathematical verification (median value). Therefore, the three essential contributions of this theoretical paper which investigates the efficacy of the noise dissolving algorithm are:

- This paper provides the exhaustive explanation of the TTSD filter algorithm (as shown in section 2).
- This paper provides the computation examples. (as shown in section 3)
- This paper provides the calculation simulation of noise apprehension correctness [33] (as shown in section 4.1) and overall comparative simulation of noise dissolving effectiveness (as shown in section 4.2) on Baboon, Resolution, F16, Girl, Lena, Mobile, Pepper, Pentagon, House for RIIN at all density (5%-90%).

The summary of this theoretical paper is presented in section 5.

2. THE THEORETICAL PERCEPTION OF TTSD FILTER FOR NOISE APPREHENSION

Define $\mathbf{x}$ as the starting portrait, which is constructed from a group of portrait dots $x_{i,j}$ at position (i,j) where the portrait intensity range is defined in $s_{min} \leq x_{i,j} \leq s_{max}$ or $[s_{min}, s_{max}]$. Define $\mathbf{y}$ as the starting point in an impulsive noisy portrait, which is constructed of a group of portrait dots $y_{i,j}$ at position (i,j). Consequently, the noisy dots $y_{i,j}$ at position (i,j) are analytically defined in (1),

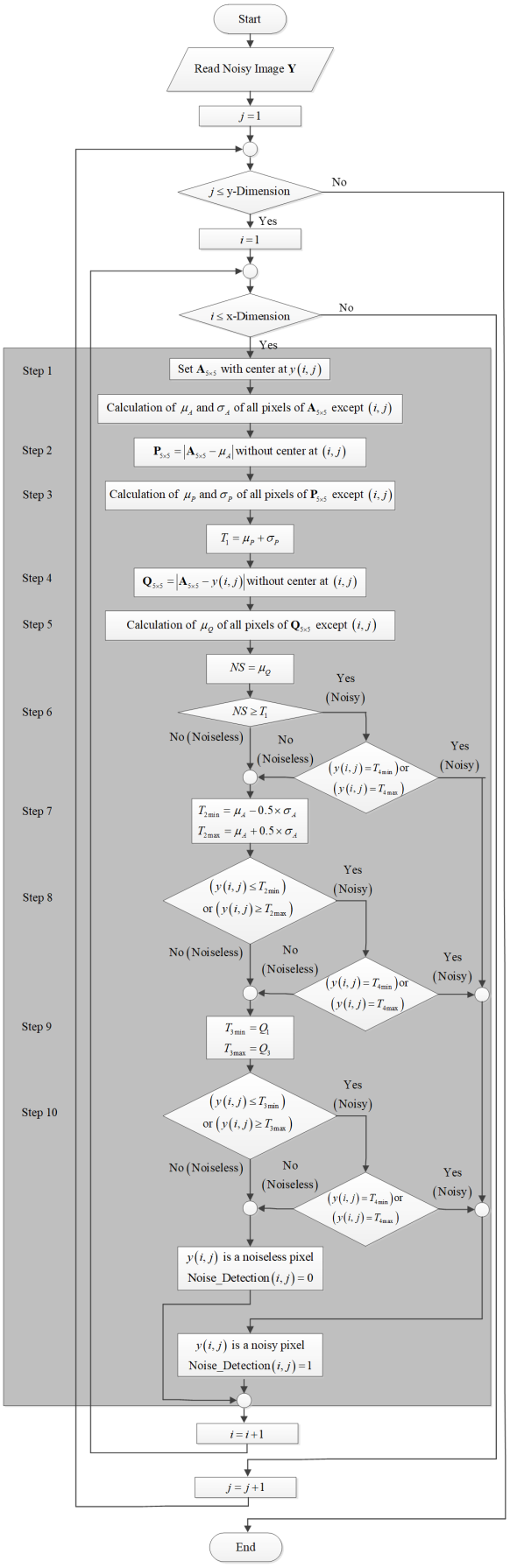

Fig.1: *Flowchart of TTSD Filter for Noise Apprehension.*

$$y_{i,j} = \begin{cases} s_{min} & \text{at probability } p \\ s_{max} & \text{at probability } q \\ x_{i,j} & \text{at probability } (1-p-q) \end{cases} \quad (1)$$

where $(p-q)$ is the noisy intensity.

For the RIIN (random intensity impulsive noise), the intensity ranges of RIIN shall be analytically defined during $s_{min} = 0$ to $s_{max} = 255$.

An exhaustive explanation of the TTSD filter algorithm for noise apprehension follows.

1. Determine the first statistic moment value (μ_A) and the second statistic moment value (σ_A) of the portrait intensity dot of the window region A, which is originally create to be $A = 5 \times 5$ at mid-position $y_{i,j}$, excluding the mid-position dot at position (i, j).
2. Determine the absolute difference p_{ij} of other nearby resident dots in the window region A with the first statistic moment value (μ_A) thus 24 determined absolute difference values (p_{ij}) is computed.
3. Determine the first statistic moment value and the second statistic moment value from the previous 24 determined absolute difference values (p_{ij}) and, later, the first constant T_1, which is the first and second statistic moment value in(2).

$$T_1 = \mu_A + \sigma_A \quad (2)$$

4. Determine the absolute difference q_{ij} of the mid-position dot $y_{i,j}$ and other 24 pixels in window region A.
5. Determine the first statistic moment value μ_q from all absolute difference q_{ij} and defined the noise signature (NS) as

$$NS = \mu_q \quad (3)$$

6. The $y_{i,j}$ is defined as noisy portrait dots if both $NS \geq T_1$ and $(0 \leq y_{i,j} \leq m$ or $255 - m \leq y_{i,j} \leq 255)$ If they are not noise go to Procedure 7.
7. Determine the second constant T_2, which is defined by the Gaussian statistic formulation (the first statistic moment value and the second statistic moment value), as

$$T_{2min} = \mu_A - 0.5 \times \sigma_A \quad (4.1)$$
$$T_{2max} = \mu_A + 0.5 \times \sigma_A \quad (4.2)$$

8. The $y_{i,j}$ are defined as noisy portrait dots if both $(y_{i,y} \leq T_{2min}$ or $y_{i,j} \geq T_{2max})$ and $(0 \leq y_{i,j} \leq m$ or $255 - m \leq y_{i,j} \leq 255)$. If they are not noise go to Procedure 9.
9. Determine the third constant T_3, which is defined by quartile statistic formulation (the median value), as

$$T_{3min} = Q_1 \quad (5.1)$$
$$T_{3max} = Q_3 \quad (5.2)$$

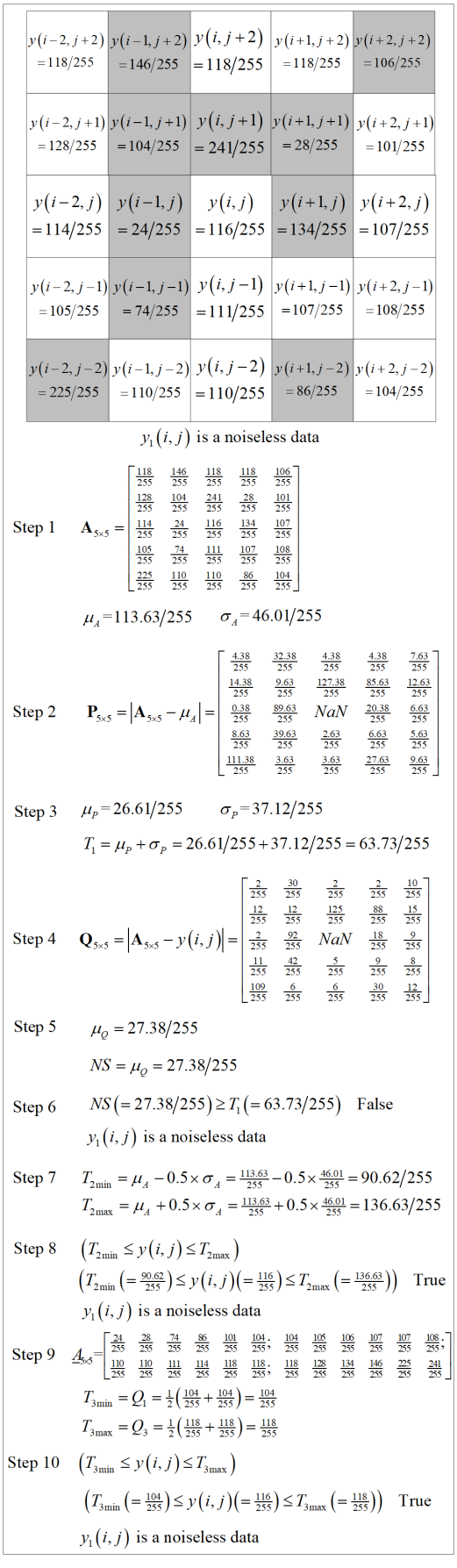

Fig.2: *Calculation of the first example operation.*

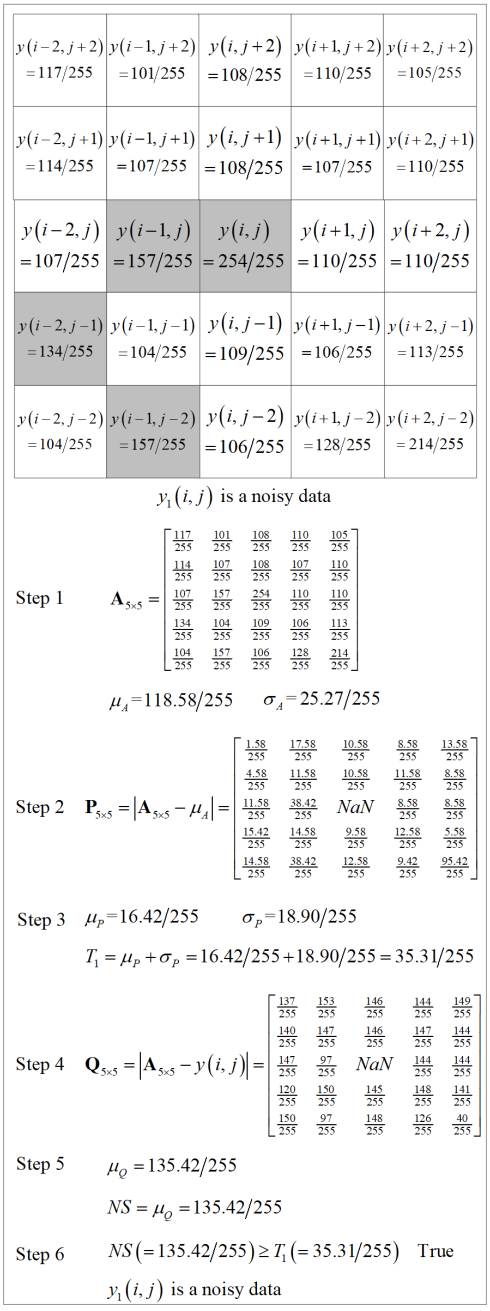

Fig.3: *Calculation of the second example operation.*

10. The $y_{i,j}$ are defined as noisy portrait dots if both ($y_{i,j} \leq Q_1$ or $y_{i,j} \geq Q_3$) and ($0 \leq y_{i,j} \leq m$ or $255 - m \leq y_{i,j} \leq 255$) otherwise $y_{i,j}$ is defined as noiseless portrait dots.

3. COMPUTATION EXAMPLES OF TTSD FILTER

This section introduces the computation case of TTSD filter for noise apprehension. The first computation case of TTSD filter for noise apprehension is shown in figure 2 for explaining the computation procedure where $y_{i,j}$ is a noise-free portrait dot ($y_{i,j} = 116$) that is not profaned from the RIIN and, consequently, the portrait dot $y_{i,j}$ is defined as a noise-free portrait dot. However, the second computation case of TTSD filter for noise apprehension is shown in figure 3 for explaining the computation procedure where $y_{i,j}$ is a noisy portrait dot ($y_{i,j} = 254$) that is profaned from the RIIN and, consequently, the portrait dot $y_{i,j}$ is defined as a noisy portrait dot.

4. CALCULATION SIMULATION

This section first provides the calculation simulation of noise apprehension correctness on nine portraits: Baboon, Resolution, F16, Girl, Lena, Mobile, Pepper, Pentagon, and House for RIIN at all densities (5%-90%) because the performance of TTSD filter was only to be investigated on three standard portraits for FIIN at density (75%-95%) in the past, as shown in section 4.1.

Second, this section provides the overall comparative simulation of noise dissolving effectiveness on eight portraits: Baboon, Resolution, F16, Girl, Lena, Mobile, Pepper, and House for RIIN at all densities (10%-90%) as shown in section 4.2.

In this experiment, the parameters of TTSD are set as window region $A = 5\times5$, $m = 255$ and other parameters (such as is $\mu_A, \sigma_A, T_1, \mu_q, T_{2min}, T_{2max}, Q_1, Q_3, T_{3min}, T_{3max}$) are automatic adaptive parameters, which are computed by Eq.(2) – Eq.(5).

4.1 Calculation Simulation of Noise Apprehension Correctness

In these computation simulation, the nine profaned portraits are used for testing the noise dissolving algorithm hinging on TTSD filter in the correctness point of view. The correctness of noisy portrait dots shall be analytically defined as shown in (6).

$$\mathrm{Acc}_{\mathrm{noisy}} = \sum_{\substack{\forall \mathrm{noisy} \\ \mathrm{pixels}}} \left(\hat{y}_{\mathrm{estimated\ noisy\ pixels}} / y_{\mathrm{noisy\ pixels}}\right) \quad (6)$$

The correctness of noise-free portrait dots shall be analytically defined as shown in (7).

$$\mathrm{Acc}_{\mathrm{noiseless}} = \sum_{\substack{\forall \mathrm{noiseless} \\ \mathrm{pixels}}} \left(\hat{y}_{\mathrm{estimated\ noiseless\ pixels}} / y_{\mathrm{noisless\ pixels}}\right) \quad (7)$$

The overall correctness of noisy and noise-free portrait dots shall be analytically defined as shown in (8).

$$\mathrm{Acc}_{\mathrm{overall}} = \left(\frac{1}{2} \sum_{\substack{\forall \mathrm{noisy} \\ \mathrm{pixels}}} \left(\frac{\hat{y}_{\mathrm{estimated\ noisy\ pixels}}}{y_{\mathrm{noisy\ pixels}}} \right) + \frac{1}{2} \sum_{\substack{\forall \mathrm{noiseless} \\ \mathrm{pixels}}} \left(\frac{\hat{y}_{\mathrm{estimated\ noiseless\ pixels}}}{y_{\mathrm{noiseless\ pixels}}} \right) \right) \quad (8)$$

The theoretical analysis of these computations of the correctness of noise-free portrait dots, noisy portrait dots and overall correctness are shown in Tables I, II and III, respectively.

Table 1: *Computation Simulation of The Apprehension Correctness of Noisy Portrait Dots.*

Tested Images	Noisy Density (%)																	
	5	10	15	20	25	30	35	40	45	50	55	60	65	70	75	80	85	90
Lena	97.59	95.28	94.40	94.20	92.71	91.31	89.87	87.57	85.23	83.58	81.19	79.28	78.05	76.56	75.34	74.31	73.24	72.73
Mobile	90.54	88.98	88.95	87.72	86.34	84.72	83.04	81.48	79.52	77.73	77.06	75.87	74.64	73.99	73.40	72.70	72.40	71.80
Pepper	95.41	95.19	94.54	92.89	92.26	90.50	88.52	86.47	84.20	82.18	80.36	78.38	76.78	75.53	74.86	73.74	72.91	72.31
Pentagon	94.61	94.18	93.57	92.81	91.78	90.56	89.29	87.58	85.78	83.89	82.06	80.23	78.56	77.16	75.84	74.73	73.64	72.90
Girl	97.34	95.93	95.58	94.24	91.40	88.84	84.70	81.80	78.50	75.93	74.46	72.21	71.10	70.48	69.72	69.36	68.68	69.27
Resolution	88.55	86.47	85.28	85.22	84.52	83.79	81.68	80.56	79.36	77.07	76.93	74.94	72.86	73.14	71.29	70.39	70.30	69.03
Baboon	90.98	91.21	89.76	88.29	87.61	86.10	84.03	82.58	81.19	79.35	77.72	77.16	75.72	74.99	73.87	73.23	72.72	72.15
House	96.34	95.24	94.00	94.28	92.76	91.60	89.98	88.11	86.71	83.89	82.38	79.36	77.88	77.08	75.40	74.38	73.65	72.08
Airplane	96.73	95.99	95.55	93.68	91.92	90.06	86.73	83.61	81.14	78.97	77.45	75.53	74.83	73.76	72.73	72.33	71.82	71.39
Average	**94.23**	**93.16**	**92.40**	**91.48**	**90.14**	**88.61**	**86.43**	**84.42**	**82.40**	**80.29**	**78.85**	**77.00**	**75.60**	**74.74**	**73.61**	**72.80**	**72.15**	**71.52**

Table 2: *Computation Simulation of The Apprehension Correctness of Noise-Free Portrait Dots.*

Tested Images	Noisy Density (%)																	
	5	10	15	20	25	30	35	40	45	50	55	60	65	70	75	80	85	90
Lena	52.91	56.38	59.19	61.18	62.76	63.64	64.28	64.63	64.74	64.68	64.23	63.51	63.11	62.19	61.89	61.38	61.16	60.80
Mobile	39.63	42.43	43.74	45.20	46.16	46.01	45.71	44.92	43.69	42.42	41.05	39.65	38.52	37.04	35.66	34.59	33.71	32.95
Pepper	55.51	58.81	60.73	61.44	61.35	60.88	59.74	58.16	56.61	55.46	53.53	52.21	50.59	49.55	48.41	48.04	47.49	47.62
Pentagon	49.05	53.62	56.67	59.15	61.24	63.08	64.71	66.42	67.63	68.60	69.55	70.11	70.58	71.16	71.25	71.52	71.60	71.56
Girl	36.27	39.88	41.85	41.01	39.07	36.51	32.67	29.58	26.21	23.66	21.87	20.53	19.53	18.71	18.26	18.05	17.71	17.54
Resolution	5.51	5.29	4.98	4.96	4.63	4.21	4.12	3.62	3.37	2.96	2.82	2.47	2.09	1.69	1.43	1.21	0.84	0.50
Baboon	45.61	48.71	50.77	51.90	52.87	52.92	52.89	53.02	53.11	52.87	53.26	53.43	53.53	53.87	53.58	53.61	53.41	52.95
House	40.20	43.88	46.99	50.22	52.59	54.77	56.47	58.14	59.93	60.64	61.34	61.93	62.00	62.01	61.85	61.22	60.77	60.40
Airplane	42.41	45.78	48.39	48.59	48.38	46.58	43.88	41.34	38.22	36.92	35.37	33.92	32.91	32.17	31.54	31.19	31.09	31.28
Average	**40.79**	**43.87**	**45.92**	**47.07**	**47.67**	**47.62**	**47.16**	**46.65**	**45.95**	**45.36**	**44.78**	**44.20**	**43.65**	**43.16**	**42.65**	**42.31**	**41.98**	**41.73**

Table 3: *Computation Simulation of The Apprehension Correctness of Overall Noisy and Noise-Free Portrait Dots.*

Tested Images	Noisy Density (%)																	
	5	10	15	20	25	30	35	40	45	50	55	60	65	70	75	80	85	90
Lena	75.25	75.83	76.80	77.69	77.74	77.48	77.08	76.10	74.99	74.13	72.71	71.40	70.58	69.38	68.62	67.85	67.20	66.77
Mobile	65.09	65.71	66.35	66.46	66.25	65.37	64.38	63.20	61.61	60.08	59.06	57.76	56.58	55.52	54.53	53.65	53.06	52.38
Pepper	75.46	77.00	77.64	77.17	76.81	75.69	74.13	72.32	70.41	68.82	66.95	65.30	63.69	62.54	61.64	60.89	60.20	59.97
Pentagon	71.83	73.90	75.12	75.98	76.51	76.82	77.00	77.00	76.71	76.25	75.81	75.17	74.57	74.16	73.55	73.13	72.62	72.23
Girl	66.81	67.91	68.72	67.63	65.24	62.68	58.69	55.69	52.36	49.80	48.17	46.37	45.32	44.60	43.99	43.71	43.20	43.41
Resolution	47.03	45.88	45.13	45.09	44.58	44.00	42.90	42.09	41.37	40.02	39.88	38.71	37.48	37.42	36.36	35.80	35.57	34.77
Baboon	68.30	69.96	70.27	70.10	70.24	69.51	68.46	67.80	67.15	66.11	65.49	65.30	64.63	64.43	63.73	63.42	63.07	62.55
House	68.27	69.56	70.50	72.25	72.68	73.19	73.23	73.13	73.32	72.27	71.86	70.65	69.94	69.55	68.63	67.80	67.21	66.24
Airplane	69.57	70.89	71.97	71.14	70.15	68.32	65.31	62.48	59.68	57.95	56.41	54.73	53.87	52.97	52.14	51.76	51.46	51.34
Average	**67.51**	**68.51**	**69.16**	**69.28**	**68.91**	**68.12**	**66.80**	**65.53**	**64.17**	**62.82**	**61.81**	**60.60**	**59.63**	**58.95**	**58.13**	**57.55**	**57.06**	**56.63**

From the computation simulation results in Table I, the noise apprehension hinging on TTSD filter has superior efficacy for RIIN due to the fact that the apprehension correctness of noisy portrait dots ($\text{Acc}_{\text{noisy}}$) is around 71%-94% for the case when noisy portrait dots are exposed as noisy portrait dots. As a result, the efficacy correctness has little relating to density of distributions.

From the computation simulation results in Table II, the noise-free apprehension hinging on TTSD filter has moderate efficacy for RIIN due to the fact that the correctness of noise-free portrait dots ($\text{Acc}_{\text{noiseless}}$) is around 41%-48% for the case when noise-free portrait dots are exposed as noise-free portrait dots. As a result, the efficacy correctness does not relate to density of distributions.

From the computation simulation results in Table III, the overall apprehension hinging on TTSD filter has good efficacy for RIIN due to the fact that the correctness of both noisy and noise-free portrait dot ($\text{Acc}_{\text{overall}}$) is about 57%-69%.

From the results in Table I - III, the noise apprehension hinging on TTSD filter has high efficacy for noisy portrait dots. However the noise reduction has moderate efficacy for noise-free portrait dots. Therefore, the noise for noise-free portrait dots must be improved in order to increase the performance of the overall noise reduction hinging on TTSD filter.

From these statistical results of TTSD based on Gaussian model and Median model, the outlier detection (in Table I) has dramatically high performance (72%-95%), but the noise-free detection performance (in Table II) has moderate performance (42%-48%). Hence, the overall detection performance (in Table III) is moderate-high performance (57%-68%). Since the Gaussian model is not desired for random value impulsive noise (RVIN), which is a non-linear distribution, the outlier distribution is higher than 30%, so the statistical model accuracy decreases. Therefore, the overall detection performance has the best performance at about 20%-25% noisy density.

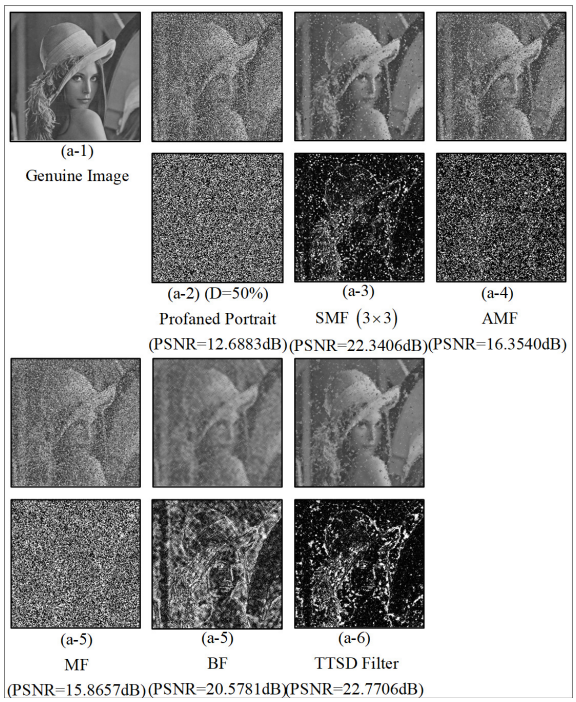

Fig.4(a): *Visual computation simulation of noise dis-solving algorithm on RIIN (Lena : 50%)*

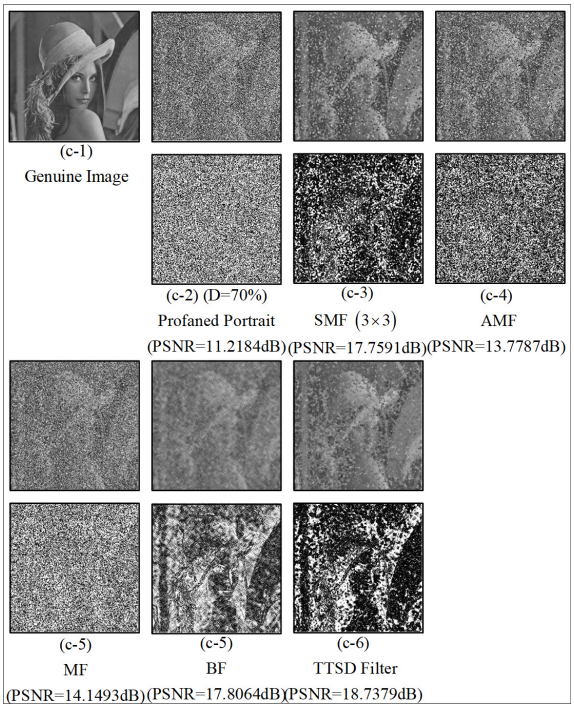

Fig.4(c): *Visual computation simulation of noise dis-solving algorithm on RIIN (Lena : 70%)*

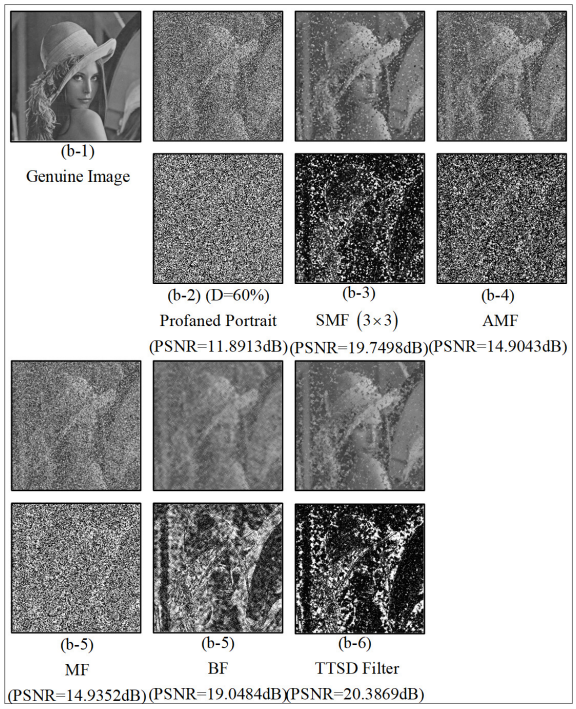

Fig.4(b): *Visual computation simulation of noise dis-solving algorithm on RIIN (Lena : 60%)*

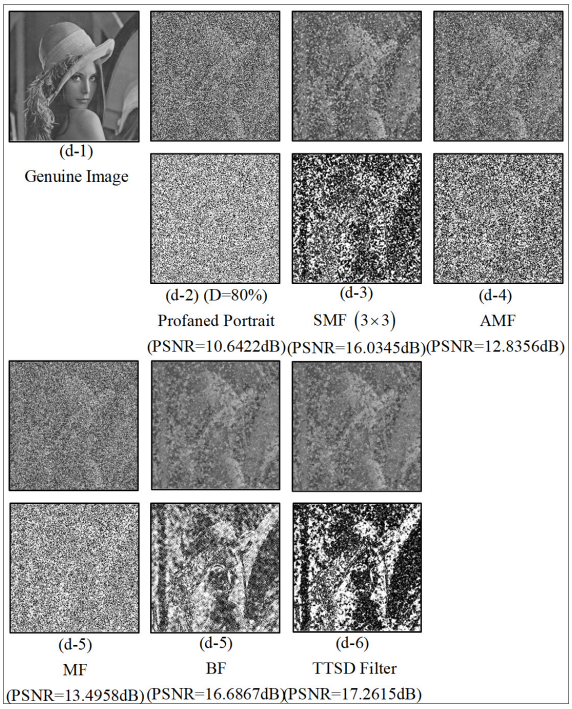

Fig.4(d): *Visual computation simulation of noise dissolving algorithm on RIIN (Lena : 80%)*

4.2 Calculation Simulation of Noise Dissolving

In this computation simulation, the efficacy of the noise dissolving algorithm that hinges on TTSD filter for RIIN (Random Intensity Impulse Noise) experiments are tested on eight guideline portraits of Baboon, Resolution, F16, Girl, Lena, Mobile, Pepper, and House in objective measurement (PSNR) as displayed in Table IV. For proving the noise dissolving efficacy, numerous state-of-art noise dissolving algorithms such as SMF (Median filter) [21], Mean/Gaussian filter [1], AMF (adaptive median filter) technique [22] and BF (Bilateral filter) [10] are comparatively implemented. Due to limited space, only partial visual comparative results of the computation simulation of noise dissolving algorithm hinging on TTSD filter and numerous state-of-art noise dissolving algorithms such as SMF (Median filter) [21], Mean/Gaussian filter [1], AMF (adaptive median filter) technique [22] and BF (Bilateral filter) [10] for Lena image under RIIN at 50%, 60%, 70% and 80% are shown in Figures 4(a), 4(b), 4(c) and 4(d), respectively. From the computation simulation results in Table IV, we conclude that the noise dissolving algorithm that hinges on TTSD filter has higher efficacy for RIIV than previous state-of-art noise dissolving algorithms. Our noise dissolving algorithm is closely equal to SMF performance because of the limitation of the noise hinges on the TTSD filter of for noise-free portrait dots.

5. CONCLUSION AND FUTURE RESEARCH

This paper investigated the efficacy of the noise dissolving algorithm hinging on TTSD (Triple Threshold Statistical Detection) filter for RIIN situation. There are three primary contributions of this theoretical paper. The first contribution of this theoretical paper is the exhaustive explanation of the TTSD filter algorithm and its computation examples. The second contribution of this paper is the calculation simulation of noise apprehension correctness on nine profaned portraits. The third contribution of this paper is an overall comparative simulation of noise dissolving effectiveness. From the computation, simulation results prove the noise apprehension hinging on TTSD filter has superior efficacy for RIIN for noise reduction.

For future research, the performance for noise-free portrait dots will be developed in order to increase the overall noise filtering hinging on TTSD filter because it has high efficacy for noisy portrait dots but only moderate efficacy for noise-free portrait dots.

ACKNOWLEDGMENT

The Portions of this research work were presented at the 42nd Electrical Engineering Conference (EECON-36), EEAAT ((Electrical Engineering Academic Association (Thailand), Greenery Resort – Khao Yai, Nakhon Ratchasima, Thailand, Oct. 2019, as "Correlation Analysis Inspection of Noise Obliteration Operation Stand on TTSD (Triple Threshold Statistical Detection) filter under Random-Valued Impulse Noise Circumstances [33]"

References

[1] R. C. Gonzalez and R. E. Woods, *Digital Image Processing*, Prentice-Hall,Upper Saddle River,NJ, USA, 2nd edition, 2002.

[2] A.S.M. Shafi and M.M. Rahman, "Decomposition of color wavelet with higher order statistical texture and convolutional neural network features set based classification of colorectal polyps from video endoscopy," *IJECE*, vol. 10, no. 3, pp.2986-2996, 2020.

[3] S. Bagchi, et.al, "Image processing and machine learning techniques used in computer-aided detection system for mammogram screening-A review," *IJECE)*, vol. 10, no. 3, pp.2336-2348, 2020.

[4] C. G. Pachón-Suescún, C. J. Enciso-Aragón and R. Jiménez-Moreno, "Robotic navigation algorithm with machine vision," *IJECE*, vol. 10, no. 2, pp.1308-1316, 2020.

[5] D. Kesrarat, et.al, "A Novel Elementary Spatial Expanding Scheme Form on SISR Method with Modifying Geman&Mcclure Function," *TELKOMNIKA*, Indonesia, vol.17, no.5, 2019.

[6] S. A. Mir and T. Padma, "Satellite Image Denoising Using Discrete Cosine Transform," *IJEEI*, vol. 5, no. 4, pp.372-375, 2017.

[7] A. M. Hasan, "A Hybrid Approach of Using Particle Swarm Optimization and Volumetric Active Contour without Edge for Segmenting Brain Tumors in MRI Scan," *IJEEI*, vol.6, no.3, pp.292-300, 2018.

[8] N. Hammouch and H. Ammor, "A confocal microwave imaging implementation for breast cancer detection," *IJEEI*, vol.7, no.2, pp.263-270, 2019.

[9] C. Bhardwaj, S. Jain and M. Sood, "Automatic Blood Vessel Extraction of Fundus Images Employing Fuzzy Approach," *IJEEI*, vol.7, no.4,, pp.757-771, 2019.

[10] V. Patanavijit, "The Bilateral Denoising Performance Influence of Window,Spatial and Radiometric Variance," *ICAICTA2015*, 2015.

[11] O. P. Verma and N. Sharma, "Intensity Preserving Cast Removal in Color Images Using Particle Swarm Optimization," *IJECE*, vol.7, no.5, pp.2581–2595, 2017.

[12] M. Hamiane and F. Saeed, "SVM Classification of MRI Brain Images for Computer-Assisted Diagnosis," *IJECE*, vol.7, no.5, pp.2555-2564, 2017.

[13] A. Khmag, S. Ghoul, S. A. R. Al-Haddad and N. Kamarudin, "Noise Level Estimation for Digital Images Using Local Statistics and Its Applications

to Noise Removal," *TELKOMNIKA*, Indonesia, vol.16, no.2, 2018.

[14] K. Arun Sai and K. Ravi, "An Efficient Filtering Technique for Denoising Colour Images," *IJECE*, vol.8, no.5, pp.3604-3608, 2018.

[15] Z. M. Ramadan, "Effect of kernel size on Wiener and Gaussian image filtering," *TELKOMNIKA*, Indonesia, vol.17, no.3, 2019.

[16] J. Na'am, et.al, "Filter technique of medical image on multiple morphological gradient (MMG) method," *TELKOMNIKA*, vol.17, no.3, 2019.

[17] B. Charmouti, et.al, "An overview of the fundamental approaches that yield several image denoising techniques," *TELKOMNIKA*, Indonesia, vol.17, no.6, 2019.

[18] B. Charmouti, et.al, "Progression approach for image denoising," *TELKOMNIKA*, Indonesia, vol.17, no.6, 2019.

[19] A. Jeelani, M.B. Veena, "Denoising using Self Adaptive Radial Basis Function," *IJEEI*, vol.7, no.4, pp.677-685, 2019.

[20] Y.Y. Al-Aboosi, et.al, "Image denosing in underwater acoustic noise using discrete wavelet transform with different noise level estimation," *TELKOMNIKA*, Indonesia, June 2020.

[21] W. K. Pratt, "Median filtering," *Tech. Rep., Image Proc. Inst., Univ. Southern California*, Los Angeles, Sep. 1975.

[22] H. Hwang and R. A. Haddad, "Adaptive median filters: new algorithms and results," in *IEEE Transactions on Image Processing*, vol.4, no.4, pp. 499-502, 1995.

[23] R. H. Chan, Chung-Wa Ho and M. Nikolova, "Salt-and-pepper noise removal by median-type noise detectors and detail-preserving regularization," in *IEEE Transactions on Image Processing*, vol.14, no.10, pp.1479-1485, 2005.

[24] Y. Dong, R. H. Chan, and S. Xu, "A Detection Statistic for Random-Valued Impulse Noise," in *IEEE Transactions on Image Processing*, vol.16, no.4, pp. 1112-1120, 2007.

[25] A. Awad, "Removal of Fixed-valued Impulse Noise based on Probability of Existence of the Image Pixel," *IJECE*, vol.8, no.4, pp. 2106-2114, 2018.

[26] V. Patanavijit, "Denoising Performance Analysis of Adaptive Decision Based Inverse Distance Weighted Interpolation (DBIDWI) Algorithm for Salt and Pepper Noise," *IJEECS*, Indonesia, Aug. 2019.

[27] V. Kishorebabu, et.al., "An adaptive decision based interpolation scheme for the removal of high density salt and pepper noise in images," *EURASIP Journal on Image and Video Processing*, 2019.

[28] V. Patanavijit and K. Thakulsukanant, "The Statistical Analysis of Random-Valued Impulse Noise Detection Techniques Based on The Local Image Characteristic: ROAD, ROLD and RORD," *IJEECS*, Indonesia, Aug. 2019.

[29] A. Abdurrazzaq, et.al, "An overview of multi-filters for eliminating impulse noise for digital images," *TELKOMNIKA*, Indonesia, vol.17, no.6, 2019.

[30] T. Matsubara, V. G. Moshnyaga, and K. Hashimoto, "A Low-Complexity and Low Power Design of 2D-Median Filter," *ECTI-CIT*, vol.5, no.2, pp.89-97 2016.

[31] Z. Yang, X. Wei, Z. Yi and G. Friedland, "Contextual Noise Reduction for Domain Adaptive Near-Duplicate Retrieval on Merchandize Images," in *IEEE Transactions on Image Processing*, vol.26, no.8, pp.3896-3910, 2017.

[32] N. Singh and U. Oorkavalan, "Triple Threshold Statistical Detection filter for removing high density random-valued impulse noise in images," *EURASIP Journal on Image and Video Pro.*, 2018.

[33] K. Thakulsukanant and V. Patanavijit, "Correlation Analysis Inspection of Noise Obliteration Operation Stand on TTSD filter under Random-Valued Impulse Noise Circumstances," *Proceeding of The 42th EECON-36*, EEAAT Thailand, Greenery Resort – Khao Yai, Nakhon Ratchasima, Thailand, Oct. 2019.

Table 4: *Computation Simulation of Noise Dissolving Algorithm on RIIN (Random Intensity Impulse Noises).*

RIIN	PSNR (dB)					
Tested Images	Noise Density	Noisy Image	Noise Dissolving Algorithm			
			SMF (3x3)	Mean (3x3)	BF (7x7)	TTSD
Lena	10	19.7193	31.1555	28.4992	23.2743	27.0308
	20	16.6527	29.7106	23.1270	20.1254	25.3046
	30	14.9222	27.5271	20.1302	18.3009	23.6748
	40	13.6990	24.9693	18.0338	16.9688	22.1054
	50	12.6883	22.3406	16.3540	15.8657	20.5781
	60	11.8913	19.7498	14.9043	14.9352	19.0484
	70	11.2184	17.7591	13.7787	14.1493	17.8064
	80	10.6422	16.0345	12.8356	13.4958	16.6867
	90	10.1515	14.5334	12.0228	12.9029	15.6162
Mobile	10	18.4574	21.4778	22.6605	21.1309	21.4697
	20	15.5151	20.8069	19.7674	18.3320	19.7203
	30	13.7727	19.7265	17.4115	16.5240	18.1395
	40	12.5299	18.5715	15.6813	15.1840	17.1620
	50	11.5304	17.1060	14.1777	14.0583	16.1111
	60	10.7497	15.5745	12.9999	13.1263	15.1169
	70	10.0875	14.2337	11.9869	12.3371	14.1821
	80	9.4794	12.9625	11.0907	11.598	13.2804
	90	8.9565	11.8224	10.2919	10.9422	12.4184
Pepper	10	19.1143	31.4270	27.4518	22.5795	26.1886
	20	16.0921	28.8665	22.3782	19.4544	24.2609
	30	14.3745	26.5900	19.4227	17.5963	22.4560
	40	13.1825	23.3362	17.2699	16.2432	20.6837
	50	12.2029	20.7731	15.6064	15.1355	19.0615
	60	11.3328	18.2128	14.0825	14.0998	17.4893
	70	10.7068	16.2565	13.0203	13.3352	16.2845
	80	10.1086	14.5768	12.0629	12.5873	15.0876
	90	9.6144	13.2495	11.2712	11.9859	14.1333
Girl	10	16.4414	31.6049	25.1361	19.8441	26.1126
	20	13.4343	28.1774	19.5726	16.5271	21.9282
	30	11.6674	23.8175	16.4551	14.5072	18.8310
	40	10.3946	19.8213	14.1249	12.9416	16.3318
	50	9.4483	16.7201	12.3872	11.7438	14.4532
	60	8.6223	14.0847	10.9357	10.6637	12.7839
	70	7.9734	12.1107	9.816	9.8004	11.4817
	80	7.3939	10.471	8.7676	8.9936	10.3334
	90	6.8638	9.156	7.9151	8.2609	9.2884

Table 5: *Computation Simulation of Noise Dissolving Algorithm on RIIN (Random Intensity Impulse Noises)(Cont.).*

RIIN	PSNR (dB)					
Tested Images	Noise Density	Noisy Image	Noise Dissolving Algorithm			
			SMF (3x3)	Mean (3x3)	BF (7x7)	TTSD
Resolution	10	17.7992	18.6254	19.3307	19.9250	20.3509
	20	14.6190	17.9190	18.1559	17.0606	17.8749
	30	12.7370	17.1231	17.1165	15.2128	16.0618
	40	11.3691	16.2456	15.6699	13.7440	14.5832
	50	10.5048	15.5229	14.6288	12.8047	13.7096
	60	9.751	14.3607	13.3621	11.9178	12.8543
	70	9.1026	13.6671	12.362	11.1682	12.1576
	80	8.4955	12.3904	11.1211	10.4038	11.3811
	90	8.0315	11.6735	10.2316	9.8152	10.8036
Baboon	10	19.0749	23.8479	24.6334	22.1068	23.1571
	20	15.9625	23.2534	21.1268	19.0599	21.5186
	30	14.1482	22.1778	18.5430	17.1939	20.3731
	40	12.9746	20.7006	16.6380	15.8863	19.1600
	50	11.9065	18.8489	14.9295	14.6632	17.7714
	60	11.1069	16.886	13.6301	13.7311	16.4986
	70	10.481	15.3038	12.6318	12.9651	15.4147
	80	9.8878	13.876	11.6611	12.2295	14.3782
	90	9.3525	12.5788	10.8606	11.5425	13.3745
House	10	19.9240	29.1907	28.1393	23.3222	26.6038
	20	16.8977	27.1182	23.6444	20.3087	24.1713
	30	14.9941	25.9646	20.2225	18.3646	22.8710
	40	13.7847	23.3376	18.0839	17.0179	21.6547
	50	12.8873	21.3497	16.5254	16.0516	20.4470
	60	11.9718	19.4005	15.0676	15.0585	19.2187
	70	11.3002	17.4083	13.9722	14.3011	18.0204
	80	10.8508	16.1719	13.1952	13.8077	17.2287
	90	10.3279	14.7128	12.349	13.2016	16.1978
F16	10	17.9926	30.6080	26.4177	21.3810	25.5989
	20	14.9461	28.2088	20.9798	18.1387	23.1623
	30	13.2327	24.4688	17.7748	16.1865	20.7702
	40	11.9817	21.5319	15.5969	14.7203	18.6289
	50	11.0346	18.5183	13.9691	13.5686	16.8527
	60	10.1911	16.0061	12.5764	12.5212	15.1914
	70	9.5278	14.0224	11.4404	11.665	13.8499
	80	8.9038	12.2414	10.4369	10.8311	12.5523
	90	8.4097	10.9895	9.6465	10.1623	11.5498

Vorapoj Patanavijit received the B.Eng., M.Eng. and Ph.D. degrees from the Department of Electrical Engineering at the Chulalongkorn University, Bangkok, Thailand, in 1994, 1997 and 2007 respectively. He has served as a full-time lecturer at Department of Electrical and Electronic Engineering, Faculty of Engineering, Assumption University since 1998 where he is currently an Associate Professor. He has authored and co-authored over 170 national/international peer-reviewed publications in Digital Signal Processing (DSP) and Digital Image Processing (DIP). He received the best paper awards from many conferences such as ISCIT2006 (2006), NCIT2008 (2008), EECON-33 (2010), EECON-34 (2011), EECON-35 (2012), EECON-43 (2020) and etc. Moreover, he is invited to be the guest speaker at IWAIT2014 and contributed the invited paper at iEECON 2014.

As a technical reviewer of international journals since 2006, he has been assigned to review over 60 journal papers (indexed by ISI). As a technical reviewer of over 40 international/national conferences since 2006, he has been assigned to review over 130 proceeding papers. He has participated in more than 8 projects and research programmed funded by public and private organizations.

He works in the field of signal processing and multidimensional signal processing, specializing, in particular, on Image/Video Reconstruction, SRR (Super-Resolution Reconstruction), Compressive Sensing, Enhancement, Fusion, Digital Filtering, Denoising, Inverse Problems, Motion Estimation, Optical Flow Estimation and Registration.

Kornkamol Thakulsukanant received the B.Eng. (Electrical Engineering) from Assumption University, Thailand in 1994, MSc. (Telecommunications and Computer Network Engineering) from London South Bank University, United Kingdom in 1997 and Ph.D. (in Electronic and Electrical Engineering) from Bristol University, United Kingdom in 2009 respectively. She served as a full-time lecturer at Faculty of Science and Technology, Assumption University since 1998 until 2014 and she has served as full-time lecturer at School of Management and Economics, Assumption University where she has been currently an Assistance Professor (in IT) since 2014.

She works in the field of Digital Signal Processing (DSP) and Digital Image Processing (DIP), specializing, in particular, on Digital Image Reconstruction/Enhancement.